ACS chemical biology

LETTERS

pubs.acs.org/acschemicalbiology

Solubilization of a Membrane Protein by Combinatorial Supercharging

Agnes Hajduczki,[†] Sudipta Majumdar,[‡] Marie Fricke,[‡] Isola A. M. Brown,[‡] and Gregory A. Weiss[†,‡,*]

[†]Department of Molecular Biology and Biochemistry and [‡]Department of Chemistry, University of California, Irvine, California 92697, United States

Supporting Information

ABSTRACT: Hydrophobic and aggregation-prone, membrane proteins often prove too insoluble for conventional *in vitro* biochemical studies. To engineer soluble variants of human caveolin-1, a phage-displayed library of caveolin variants targeted the hydrophobic intramembrane domain with substitutions to charged residues. Anti-selections for insolubility removed hydrophobic variants, and positive selections for binding to the known caveolin ligand HIV gp41 isolated functional, folded variants. Assays with several caveolin binding partners demonstrated the successful folding and functionality by a solubilized, full-length caveolin variant selected from the library. This caveolin variant allowed assay of the direct interaction between caveolin and cavin. Clustered along one face of a putative helix, the solubilizing mutations suggest a structural model for the intramembrane domain of caveolin. The approach provides a potentially general method for solubilization and engineering of membrane-associated proteins by phage display.

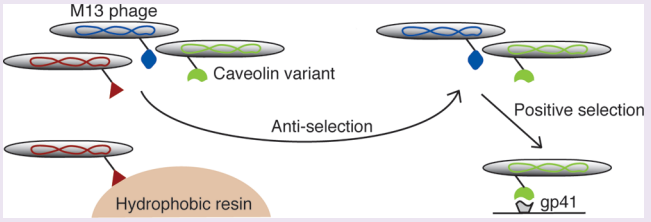

Membrane-associated proteins contribute essential functions to the cell, including energy generation, communication, transportation, and sensing. The hydrophobic regions of membrane proteins force them into the lipophilic environment of membranes, and such proteins typically aggregate upon removal from the membrane.[1] The latter property makes structural and biophysical studies of membrane-associated proteins extremely challenging. Thus, in contrast to the thousands of soluble protein structures deposited in the Protein Data Bank, only about 200 membrane protein structures have been solved to date.[2] The solubilization of functional membrane proteins through mutations to the transmembrane domain remains relatively unexplored as a solution to this challenge.

Largely conserved among higher eukaryotes, human caveolin-1 is one of three members of the caveolin family.[3,4] Most frequently expressed in adipocytes and endothelial cells, caveolin-1 (hereafter referred to as caveolin) plays key roles in signal transduction and the initiation of endocytosis.[5] Although involved in a variety of diseases including Alzheimer's disease, muscular dystrophy, cancer, diabetes, obesity, and asthma,[6] the structure of the 178-residue, membrane-associated caveolin remains undetermined.

Caveolin, associated with detergent-insoluble lipid rafts, is a monotopic membrane protein.[6] Thus, the region between residues 102 and 134 inserts into one leaflet of the plasma membrane, and N- and C-termini remain in the cytoplasm. Oligomerized caveolin in complex with additional proteins causes invaginations in the plasma membrane, termed caveolae.[7] Signaling molecules bind to caveolin, and cluster in high concentrations at caveolae.[8] The caveolin scaffolding domain (CSD), comprised of caveolin residues 81−101 binds to and inhibits endothelial nitric oxide synthase (eNOS) and protein kinase A (PKA).[9−11] HIV gp41, the viral envelope protein responsible for membrane fusion during viral entry, also interacts with the CSD.[12,13]

Structural studies, using X-ray crystallography or NMR, generally require large quantities of sometimes isotopically enriched, purified protein, which is most readily produced by protein overexpression in *E. coli*. As a result, optimizing expression of mammalian proteins in bacteria attracts strong interest. However, prokaryotes have lipid bilayer compositions different from those of eukaryotes and lack eukaryotic protein processing machinery; thus, bacteria often struggle with the overexpression, folding, assembly, and stabilization of eukaryotic membrane proteins.

Though success in the overexpression of membrane proteins has been reported,[14,15] such proteins often trigger a bacterial reaction similar to a stress response, and the aggregated proteins accumulate in inclusion bodies.[16] Recovery of proteins from inclusion bodies typically involves complete denaturation of the aggregated proteins with harsh denaturants,[17] followed by time-consuming and only occasionally successful refolding protocols. In extreme cases, for example, with caveolin, the hydrophobic protein obstructs the bacterial protein synthesis machinery, and the protein expression fails entirely. Bovine caveolin fused to glutathione *S*-transferase (GST) expresses to levels sufficient for immunoblot detection in bacteria,[18,19] but purification of caveolin in sufficient quantities for biophysical and structural characterization has not been reported.

Received: June 14, 2010
Accepted: December 30, 2010
Published: December 30, 2010

Table 1. Expression Profile of Various Caveolin Selectants[a]

Clone ID	Intra-membrane sequence	Expression in inclusion body	Soluble expression (MBP-fusion)	Mutations
Library design	LLSALFGIPMALIWGIYFAILSFLHIWAVVPCI RD K DKR KDD KR DK KR ED Y N HN N Y N YQ N DE V V V VM			
Wt cav	LLSALFGIPMALIWGIYFAILSFLHIWAVVPCI	–	–	0
cav1	LLSARFGIPMALIWGIYFAILSFLHIWAVVPCI	–	n/d	1
cav2	LLSARDGIPMAVIWGIYFAILSFLHIWAVVPCI	–	n/d	3
cav3	LLSARVGIPMALKWGIDFAILSFLHKWAVVPCI	–	n/d	5
cav4	LLSALFGIPMAHNWGIYFANLSVKHIWAVEPCI	–	n/d	6
cav5	LLSALDGIPMALKWGIDFANLSFMHNWAVVPCI	–	n/d	6
cav6	LLSARFGIPMAHIWGKDFAILSDMHIWAVVPCI	–	n/d	6
cav7	LLSALYGIPMAHNRGIYDAILSFQHIWAVEPCI	–	n/d	7
cav8	LLSALFGIPMALKWGNYDAKLSVMHKWAVVPCI	–	n/d	7
cav9	LLSARDGIPMALIWGIDDANRSYKHNWAVVPCI	++	++	9
cav10	LLSARDGIPMAVNWGKDDANRSFLHIWAEEPCI	+++	–	11
cav11	LLSARDGIPMAVNRGIDFAKLSDKHNRAVDPCI	+++	++	12
cav12	LLSARDSNPMADKRGNDVAILSVQHIRAVVPCI	++	–	13
cav13	LLSALDGIPMAVNRGKDVAIRSFMHNRTDVPCI	++	–	13
cav14	LLSARDGQTDGSQMGHLRRHTL*	+++	n/d	n/d
cav15	LLSARVGQTDGTHLGH*	+++	n/d	n/d

[a] Black letters indicate wild-type residues, red letters designate mutations encoded in the library, and the residues in blue are spontaneous mutations that arose during propagation in *E. coli*. Underlined residues were selected in at least four of the five full-length variants that expressed in *E. coli*, which can identify residues contributing favorably to protein solubility and/or stability. Abbreviations indicate wild-type (wt), expression levels (+), no expression (−), not determined (n/d), and stop codons (*).

Our laboratory has previously reported successful display of full-length caveolin and other membrane proteins on M13 filamentous bacteriophage.[20] The helper phage used for membrane protein display is a modified version of the conventional M13-KO7, termed KO7^{+}; a AKAS tetrapeptide insertion near the solvent-exposed N-terminus of the major coat protein disrupts a group of negative charges by adding a positively charged lysine.[21] This first example of membrane protein display enables phage-based combinatorial mutagenesis, to engineer new activities into membrane proteins. Here, we report selections to solubilize caveolin and enable bacterial overexpression of the large quantities required for biophysical and structural studies. In a related approach targeting the surface of an insoluble protein, Liu and co-workers identified 29 solvent exposed residues in GFP on the basis of the crystal structure, which were mutated to lysines or arginines to achieve increased solubility while retaining fluorescence.[22] In another approach, computational design has been used to generate a soluble variant of the potassium channel KcsA.[23] In the present study, the unknown structure of caveolin required a combinatorial approach to introduce solubilizing mutations into the intramembrane domain (IMD) of caveolin.

Full-length caveolin cannot be overexpressed in *E. coli* using conventional methods, such as varying induction conditions including IPTG concentration and growth temperature (Supplementary Figure 1). Fusion of full-length caveolin to maltose binding protein (MBP)[24] and introduction of 2−4 potentially solubilizing mutations (*e.g.*, lysine and arginine substitutions) in the hydrophobic IMD (constructs 5, 6, 7, and 8 in Supplementary Figure 1, panel a) does not improve expression levels. Only one of a large number of caveolin constructs resulted in successful overexpression of caveolin in *E. coli*. Consisting of caveolin residues 1−104, this construct of caveolin, termed cav(1−104), is truncated to eliminate the IMD and C-terminal regions. Cav(1−104) expresses only insoluble protein in the inclusion body fraction of lysed bacteria (Supplementary Figure 1, panel b); thus, cav(1−104) requires denaturation and detergent-based refolding. Since the removal of the IMD renders caveolin sufficiently soluble for overexpression, though as an aggregation-prone protein, the hydrophobicity of the IMD likely prevents its overexpression in *E. coli*. This observation provides an empirical foundation for introducing mutations into the IMD to convert the full-length protein into a soluble construct for overexpression.

Site-directed mutagenesis with degenerate oligonucleotides programmed the phage-displayed library of caveolin variants. The library design targeted the most hydrophobic IMD side chains with codons substituting a mixture of the wild-type residue and charged residues, either Lys/Arg or Glu/Asp (Table 1). As a result of degeneracy of the genetic code, some positions also encoded a third or fourth amino acid. The theoretical diversity of the resulting naïve library was deliberately limited to a modest 7×10^7 different variants to ensure complete coverage of all possible combinations by the phage-displayed library, including wild-type, in every position. Indeed, the resultant library had a practical diversity of 4.3×10^9 as measured by phage titers.

Five rounds of serial negative and positive selections were used to isolate soluble caveolin variants from the phage-displayed library of caveolin variants (Figure 1, panel a). During the negative or anti-selections, caveolin variants binding to hydrophobic interaction chromatography resin (butyl sepharose) were removed from the library; this step can subtract hydrophobic, unfolded, and aggregation-prone variants.[25] After filtration to remove the resin with the bound phage, the less hydrophobic variants were recovered from the flow-through and were next incubated with surface-bound gp41 ectodomain. This second, positive selection step ensured that the selected variants are properly folded and could bind to gp41, a known caveolin function. During each round, increasing both the salt concentration and the number of washes for the negative and positive

dx.doi.org/10.1021/cb1001729 |*ACS Chem. Biol.* 2011, 6, 301–307

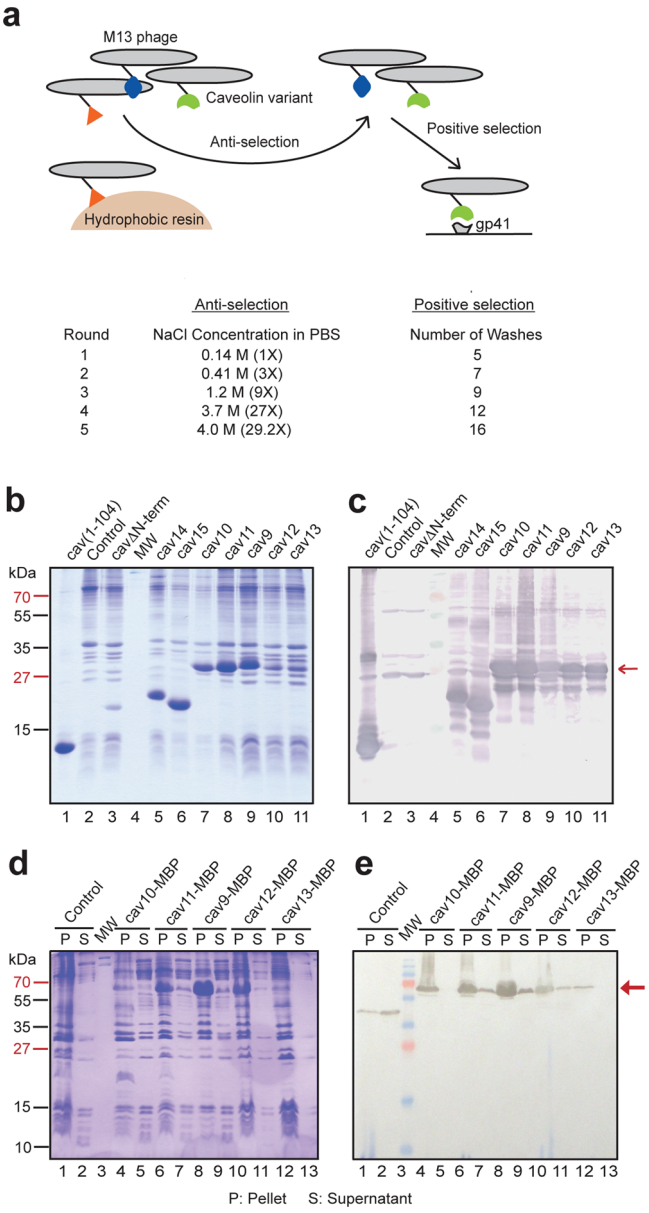

Round	Anti-selection: NaCl Concentration in PBS	Positive selection: Number of Washes
1	0.14 M (1X)	5
2	0.41 M (3X)	7
3	1.2 M (9X)	9
4	3.7 M (27X)	12
5	4.0 M (29.2X)	16

Figure 1. Selection, design, and expression of caveolin selectants. (a) Solubility selections using a phage-displayed library of caveolin intramembrane domain (IMD) variants. The anti-selection eliminates aggregation-prone, hydrophobic variants binding to hydrophobic interaction chromatography resin. Then, a positive selection step isolated variants binding to gp41. The increased salt concentration and washes during the selections increase the stringency of the selections. (b) SDS-PAGE and (c) Western blot of *E. coli* crude lysates expressing caveolin variants, using an antibody that recognizes the N-terminus of caveolin. Purified cav(1−104) in lane 1 is a positive control. The negative control in lane 2 is the lysate fraction of *E. coli* carrying the empty expression vector. An additional control in lane 3 shows expression of a 17 kDa caveolin variant (cavΔN-term) that lacks the antibody recognition site. The red arrow indicates the expected size of full-length caveolin fused to a His_6 tag (~24.9 kDa). (d) SDS-PAGE and (e) Western blot of *E. coli* lysates expressing full-length caveolin variants with a N-terminal MBP fusion having the expected size indicated by the red arrow (~64.5 kDa). An antibody specific for MBP detects the presence of the overexpressed proteins. The pellet fraction (P) represents the insoluble proteins after cell lysis and centrifugation, and S indicates the soluble fraction. The control in lanes 1 and 2 is lysate from *E. coli* cells expressing only MBP.

selections, respectively, increased the selection stringency for each subsequent selection round.

PCR amplification of the caveolin gene in the M13 phagemid after each round of selection identified a truncated species of the caveolin ORF emerging in round three, which dominated the population of caveolin variants by round five (Supplementary Figure 2, panel a). DNA sequencing revealed the deletion of the IMD and most, but not all, of the C-terminal domain from this truncated variant of caveolin. Emergence of truncated variants during selections is not uncommon, since the phage displaying smaller proteins often have an inherent growth advantage. The lack of IMD in the truncated caveolin variants further confirms that the hydrophobicity of the IMD is the major obstacle to caveolin expression in *E. coli* for both soluble expression (Supplementary Figure 1) and as a fusion to the phage coat protein P8.

To examine individual caveolin variants, selectants from the fourth round of selection were subcloned into a protein overexpression vector (pET28c). Truncated variants were removed from this screening population during subcloning. The annealing region of the PCR primers for this subcloning required inclusion of the C-terminal region (Supplementary Figure 2, panel b).

Individual caveolin variants were screened for overexpression in *E. coli*. Among the 44 variants screened, seven clones produced moderate amounts of protein using a standard expression vector, pET28 (Figure 1, panel b, lanes 5−11). Cav14 and cav15 expressed truncated proteins lacking most of the IMD and the C-terminal domain. The high levels of expression of these truncated variants further suggests that the presence of the hydrophobic IMD sequence is the main obstacle for the expression of full-length caveolin in *E. coli*. Five selectants resulted in a protein with the size expected for full-length caveolin (Figure 1, panel b, lanes 7−11). The overexpressed proteins were confined to the inclusion body fraction (Supplementary Figure 3); however, fusion of these full-length caveolin variants to the solubility enhancing maltose-binding protein (MBP) allowed consistent overexpression of one variant (cav11) as a soluble protein (Figure 1, panel c, lane 7). The five full-length variants capable of overexpression included 9−13 solubilizing amino acid mutations in the IMD (Table 1). These variants with improved solubility included side chains contributing favorably to protein solubility, stability, or both. All five caveolin variants included an aspartic acid residue at position 107 and 118, and four of the five variants included an arginine at residue 106 and an isoleucine at position 109.

In contrast, eight other caveolin variants with only 1−7 mutations in their IMDs failed to express in *E. coli* (Table 1). In cav11, the variant with the most improved solubility, 12 of the 17 targeted positions were mutated. The experiment demonstrates the requirement for extensive mutations in the IMD for solubilizing a membrane-associated protein. About 10 mg of soluble cav11-MBP can be recovered from 1 L of *E. coli* culture (Supplementary Figure 4). Size-exclusion chromatography confirmed that the cav11-MBP forms oligomers as expected (Supplementary Figure 5).

Enzyme-linked immunosorbent assays (ELISAs) with cav11-MBP and caveolin binding partners, both known and putative, demonstrate that the soluble caveolin variant is properly folded and functional. As expected cav11-MBP binds well to its previously identified ligands, including the gp41 ectodomain, protein kinase A (PKA), and cav(1−104) (Figure 2, panel a). The latter result further demonstrates that solubilized caveolin retains the capability to form oligomers. In negative controls, MBP fails to bind the target

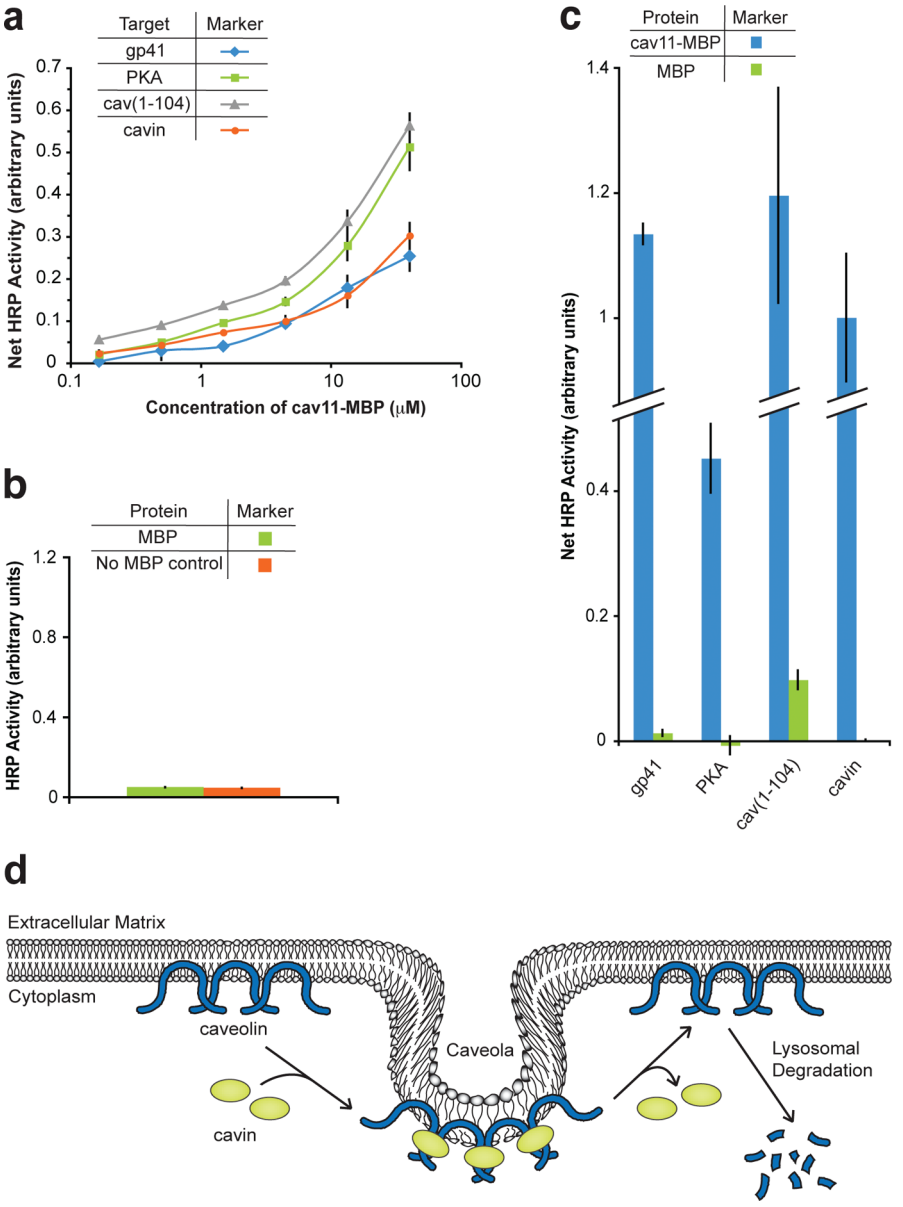

Figure 2. Binding by the solubilized full-length caveolin variant (cav11-MBP) to cavin and three other binding partners. (a) In this ELISA, cav11-MBP binds to known binding partners gp41 ectodomain, protein kinase A (PKA), or truncated caveolin, cav(1−104), and cavin. Binding to the blocking agent (nonfat milk) was subtracted to provide the net HRP activity. Cav11-MBP binds to all four targets. (b) As negative controls, MBP fails to the blocking agent used in panel a (nonfat milk), and no signal is observed for control wells with MBP omitted. (c) In addition, cav11-MBP (4 μM) binds well to the target proteins when BSA is used as a blocking agent; the negative control, MBP (4 μM), fails to bind to the target proteins. Error bars indicate standard deviation (n = 3). (d) The role of cavin in caveolae formation. Membrane bending and formation of caveolae requires the interaction of cavin with caveolin. Results reported here demonstrate that caveolin can bind directly to cavin. Dissociation of cavin destabilizes the caveolae, and caveolin can then be targeted for lysosomal degradation. Schematic adapted from ref 34.

proteins and nonfat milk (Figure 2, panels b and c), which demonstrates the specificity of the assayed binding interactions.

In addition, cav11-MBP binds directly to cavin, a protein also known as Cav-p60 or Polymerase I and transcript release factor (PTRF) (Figure 2, panel a). Though a soluble protein, cavin also localizes to the plasma membrane.[26,27] Co-immunoprecipitation from unpurified cell lysates and FRET/FLIM measurements suggested that caveolin and cavin form multimeric complexes with other proteins in the caveolae.[27] Direct binding, however, between cavin and caveolin has been suggested but not demonstrated previously. Thus, the results reported here add to the model of dynamic caveolae formation regulated by direct cavin binding to caveolin; the dissociation of cavin then causes instability of caveolae and consequent degradation of caveolin (Figure 2, panel d). The relative binding affinity of cav11-MBP for the four binding partners appears roughly comparable under the assay conditions.

The mutations required for caveolin solubilization also support a structural model of an α-helix for the IMD of caveolin. Instead of the amphipathic character observed for the in-plane helices of other monotopic proteins,[28−30] the putative caveolin IMD helix is hydrophobic with one face featuring aromatic and the other aliphatic side chains (Figure 3, panel b). Aromatic side chains in intramembrane helices, especially tryptophan and tyrosine, are often located at the membrane interface region.[31,32]

dx.doi.org/10.1021/cb1001729 |ACS Chem. Biol. 2011, 6, 301–307

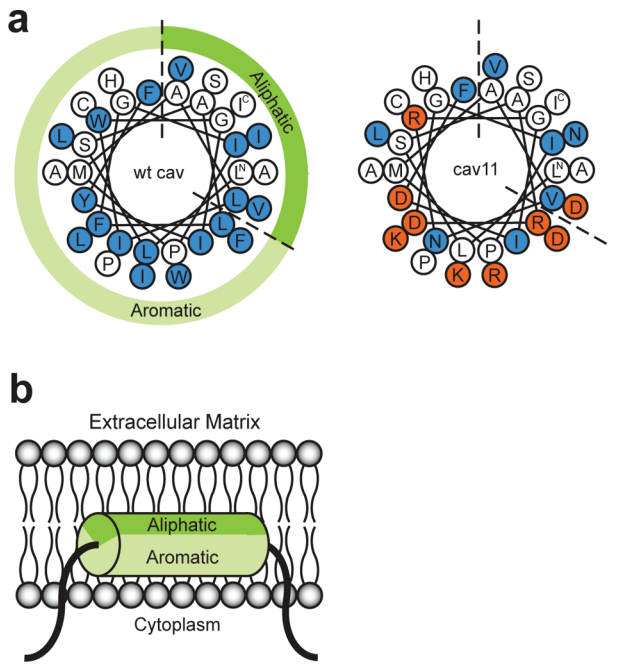

Figure 3. Predicted membrane topology of the caveolin IMD. (a) Helical wheel representations of the IMDs of wild-type (wt) caveolin and cav11. The aliphatic and aromatic faces of the helix are shown, and N and C superscripts indicate the N- and C-termini. Residues in blue were targeted for mutagenesis in the library. Orange residues designate positions with charged residues substituted for the soluble variant. (b) Proposed membrane topology of the wild-type caveolin IMD α-helix.

In this model for an in-plane α-helix of the caveolin IMD, the aliphatic side chains interact with the fatty acid tails of the membrane lipids, and the aromatic side chains form cation-π interactions with the primary and quaternary amines at the membrane interface region. This model suggests that large oligomers of caveolin could bend the plasma membrane by wrapping the membrane around the aromatic two-thirds of the putative IMD α-helix. Additionally, the solubilizing mutations target the aromatic face of the putative α-helix (Figure 3, panel a). Thus, solubilization converts the IMD from a fully hydrophobic to an amphipathic α-helix.

In summary, we report a method for the solubilization of a human membrane protein using a new type of phage display. Because of its hydrophobic character, caveolin-1 was previously inaccessible for large-scale expression in *E. coli*. *In vitro* evolution resulted in a soluble caveolin variant. This variant expresses in large quantities using standard bacterial expression protocols. Binding assays with three binding partners confirmed the correct functioning of the solubilized caveolin. In addition, binding assays demonstrated the direct interaction between caveolin and cavin. Since at the cell membrane cavins and caveolins form large multimeric complexes with other proteins and lipids, this interaction could only be elucidated using purified proteins, such as solubilized caveolin. Therefore, the reported experiments demonstrate the power of phage-displayed membrane proteins for engineering and dissecting membrane proteins.

METHODS

Construction and Isolation of the Caveolin Phage Display Library. The phage-displayed library of caveolin-1 variants was generated by site-directed mutagenesis[33] with degenerate oligonucleotides designed to encode the variants described in Table 1. The template for the library was the wild-type caveolin gene inserted into the phage display vector as described previously.[20] The DNA encoding the library of variants were desalted using the QIAQuick Gel Extraction Kit from Qiagen and electroporated into electrocompetent *E. coli* SS320 cells. Following 20 min of incubation at 37 °C in SOC media, a 10 μL aliquot was removed from the 25 mL of recovery culture, serially diluted in 2YT, and plated on LB and LB/carbenicillin plates to establish the library titer. The recovery culture was infected with KO7^{+} helper phage at a concentration of ~1.5 × 10^{10} phage/μL and shaken for 1 h at 37 °C. The entire culture was then transferred to 500 mL of 2YT containing 50 μg/mL carbenicillin and 20 μg/mL kanamycin and shaken overnight at 37 °C. The phage displaying the caveolin library were isolated using PEG-NaCl precipitation and dissolved in PBS (2 mL).

Selections for Solubility and Binding to HIV gp41. For the anti-selection step, 2 mL of the phage solution was mixed with 667 μL of hydrophobic interaction chromatography resin containing butyl sepharose (GE Healthcare). Following a 1 h incubation on a shaker at RT, the solution was filtered, and the unbound phage were collected from the flow-through before reprecipitation and suspension in PBS. For rounds 2, 3, 4, and 5, the phage solution had increasing concentrations of NaCl: 3×, 9×, 27×, and 29.2×, respectively, relative to the concentration of NaCl in PBS. Next, the positive selection used a format similar to the phage display ELISA. Wells of 96-well microtiter plates (Nunc) were coated with 15 μg/mL gp41 ectodomain (see below for construct details and expression protocol) in 100 μL of 50 mM Na_2CO_3, pH 9.6, and incubated overnight at 4 °C on a shaker. After removal of the coating solution, 400 μL of a solution of 0.2% w/v bovine serum albumin (BSA) in PBS was used to block the wells for 30 min on a shaker at RT. The plate was then washed three times with 200 μL of 0.05% Tween-20 in PBS. Phage were added to the wells in a buffer containing 0.2% w/v BSA, 0.05% Tween-20 in PBS. After a 1 h incubation on a shaker at RT, the wells were washed with 0.05% Tween-20 in PBS. The number of washes were 5, 7, 9, 12, and 16 for the five selection rounds, respectively. The bound phage were eluted by addition of 100 μL of 0.1 M HCl with vigorous shaking at RT for 5 min. The solution was neutralized with 33 μL of 1 M Tris-HCl, pH 8.0 and collected from the wells into a 5 mL tube. One milliliter of the eluted phage were used to infect 10 mL of log phase *E. coli* XL-1 Blue cells before incubation for 1 h at 37 °C. Helper phage was added to a final concentration of ~1.5 × 10^{13} pfu/mL, and after 1 h of incubation, the culture was transferred to 200 mL of 2YT containing 50 μg/mL carbenicillin and 20 μg/mL kanamycin and shaken overnight at 37 °C.

Expression Constructs. To express the gp41 ectodomain construct, residues 546−578 and 624−655 attached by a glycine-rich linker were subcloned into the pET28c vector. The truncated caveolin construct encodes caveolin residues 1−104 with a N-terminal TEV protease site (ENLYFQG) as a linker to a His-tag in the pET28c vector between the *Bam*HI and *Eco*RI restriction sites. The gene for the PKA catalytic subunit alpha was purchased from Addgene. The cavin (PTRF) gene, encoded in the pET28c vector described above, contained a R183H mutation not expected to change the properties of the protein. The selected caveolin variants from round 4 were PCR-amplified using primers encoding *Bam*HI and *Eco*RI restriction sites on their overhangs. The resulting PCR products were subcloned as a population into the modified pET28c vector between the *Eco*RI and *Sal*I sites, which contains the gene for *E. coli* maltose-binding protein (MBP) between the NheI and *Eco*RI restriction sites.

Protein Overexpression and Purification. The protein overexpression was performed using *E. coli* BL21(DE3) cells. The buffers were typically based on a common lysis buffer (300 mM NaCl, 50 mM NaH_2PO_4 pH 8.0) with the exception of PKA in which NaCl in the buffers was replaced with KCl. The crude lysate was incubated with the nickel-NTA resin for 2 h at 4 °C in the presence of lysis buffer with 10 mM 2-mercaptoethanol. After collection of the flowthrough, the

column was washed with wash buffer (lysis buffer containing 20 mM imidazole). The bound proteins were eluted with lysis buffer containing 250 mM imidazole. The purity of the proteins was monitored by SDS-PAGE using 15% polyacrylamide gels (Supplementary Figure 4). The nickel-affinity purified protein was dialyzed against PBS, concentrated, and further purified by size-exclusion chromatography.

Western Blots. Samples of *E. coli* lysates expressing the caveolin variants were electrophoretically separated by SDS-PAGE before transfer to nitrocellulose membranes. The membranes were blocked with 5% nonfat milk (NFM) in 100 mM Tris (pH 9.5), 100 mM NaCl, 5 mM $MgCl_2$. The primary antibodies were either rabbit anti-caveolin-1 or mouse anti-MBP. For the anti-caveolin-1, an alkaline phosphatase conjugated secondary antibody was used, and for the anti-MBP antibody, a horseradish peroxidase-conjugated secondary antibody was used. The detection reagents were 5-bromo-4-chloro-3′-indolyphosphate *p*-toluidine with nitro-blue tetrazolium chloride (BCIP/NBT) and 4-chloro-1-naphthol with 3,3′-diaminobenzidine, tetrahydrochloride (CN/DAB), respectively.

ELISAs. The target proteins coated the wells at concentrations of 15 μg/mL. Following blocking with a 0.2% solution of bovine serum albumin (BSA) or 0.2% (NFM) in PBS, the indicated concentrations of cav11-MBP or equivalent molar concentrations of MBP were added to the wells in PBS containing either 0.2% BSA or 0.2% NFM. A MBP-specific primary antibody (Mouse anti-MBP from Sigma) and horseradish peroxidase-conjugated secondary antibody (anti-Mouse-HRP from Sigma) detected presence of bound protein. A solution of *o*-phenylenediamine (20 mM) was used to detect HRP activity.

■ ASSOCIATED CONTENT

Supporting Information. This material is available free of charge *via* the Internet at http://pubs.acs.org.

■ AUTHOR INFORMATION

Corresponding Author

*Tel: 1-949-824-5566. Fax: 1-949-824-9920. E-mail: gweiss@uci.edu.

■ ACKNOWLEDGMENT

We thank G. Eldridge, J. Lamboy, R. Lathrop, S. White, and D. Tobias for helpful discussions. This work was supported by the National Institutes of Health, National Institute of General Medical Sciences (R01 GM078528-01).

■ REFERENCES

(1) Rees, D. C., Komiya, H., Yeates, T. O., Allen, J. P., and Feher, G. (1989) The bacterial photosynthetic reaction center as a model for membrane proteins. *Annu. Rev. Biochem. 58*, 607–633.

(2) White, S. H. (2004) The progress of membrane protein structure determination. *Protein Sci. 13*, 1948–1949.

(3) Tang, Z., Okamoto, T., Boontrakulpoontawee, P., Katada, T., Otsuka, A. J., and Lisanti, M. P. (1997) Identification, sequence, and expression of an invertebrate caveolin gene family from the nematode *Caenorhabditis elegans*. Implications for the molecular evolution of mammalian caveolin genes. *J. Biol. Chem. 272*, 2437–2445.

(4) Spisni, E., Tomasi, V., Cestaro, A., and Tosatto, S. C. (2005) Structural insights into the function of human caveolin 1. *Biochem. Biophys. Res. Commun. 338*, 1383–1390.

(5) Razani, B., Woodman, S. E., and Lisanti, M. P. (2002) Caveolae: from cell biology to animal physiology. *Pharmacol. Rev. 54*, 431–467.

(6) Cohen, A. W., Hnasko, R., Schubert, W., and Lisanti, M. P. (2004) Role of caveolae and caveolins in health and disease. *Physiol. Rev. 84*, 1341–1379.

(7) Tran, D., Carpentier, J. L., Sawano, F., Gorden, P., and Orci, L. (1987) Ligands internalized through coated or noncoated invaginations follow a common intracellular pathway. *Proc. Natl. Acad. Sci. U.S.A. 84*, 7957–7961.

(8) Sargiacomo, M., Sudol, M., Tang, Z., and Lisanti, M. P. (1993) Signal transducing molecules and glycosyl-phosphatidylinositol-linked proteins form a caveolin-rich insoluble complex in MDCK cells. *J. Cell Biol. 122*, 789–807.

(9) Garcia-Cardena, G., Fan, R., Stern, D. F., Liu, J., and Sessa, W. C. (1996) Endothelial nitric oxide synthase is regulated by tyrosine phosphorylation and interacts with caveolin-1. *J. Biol. Chem. 271*, 27237–27240.

(10) Razani, B., Rubin, C. S., and Lisanti, M. P. (1999) Regulation of cAMP-mediated signal transduction via interaction of caveolins with the catalytic subunit of protein kinase A. *J. Biol. Chem. 274*, 26353–26360.

(11) Levin, A. M., Murase, K., Jackson, P. J., Flinspach, M. L., Poulos, T. L., and Weiss, G. A. (2007) Double barrel shotgun scanning of the caveolin-1 scaffolding domain. *ACS Chem. Biol. 2*, 493–500.

(12) Hovanessian, A. G., Briand, J. P., Said, E. A., Svab, J., Ferris, S., Dali, H., Muller, S., Desgranges, C., and Krust, B. (2004) The caveolin-1 binding domain of HIV-1 glycoprotein gp41 is an efficient B cell epitope vaccine candidate against virus infection. *Immunity 21*, 617–627.

(13) Huang, J. H., Lu, L., Lu, H., Chen, X., Jiang, S., and Chen, Y. H. (2007) Identification of the HIV-1 gp41 core-binding motif in the scaffolding domain of caveolin-1. *J. Biol. Chem. 282*, 6143–6152.

(14) Grisshammer, R. (2006) Understanding recombinant expression of membrane proteins. *Curr. Opin. Biotechnol. 17*, 337–340.

(15) Massey-Gendel, E., Zhao, A., Boulting, G., Kim, H. Y., Balamotis, M. A., Seligman, L. M., Nakamoto, R. K., and Bowie, J. U. (2009) Genetic selection system for improving recombinant membrane protein expression in *E. coli*. *Protein Sci. 18*, 372–383.

(16) Miroux, B., and Walker, J. E. (1996) Over-production of proteins in Escherichia coli: mutant hosts that allow synthesis of some membrane proteins and globular proteins at high levels. *J. Mol. Biol. 260*, 289–298.

(17) Lim, W. K., Rosgen, J., and Englander, S. W. (2009) Urea, but not guanidinium, destabilizes proteins by forming hydrogen bonds to the peptide group. *Proc. Natl. Acad. Sci. U.S.A. 106*, 2595–2600.

(18) Ju, H., Zou, R., Venema, V. J., and Venema, R. C. (1997) Direct interaction of endothelial nitric-oxide synthase and caveolin-1 inhibits synthase activity. *J. Biol. Chem. 272*, 18522–18525.

(19) Ghosh, S., Gachhui, R., Crooks, C., Wu, C., Lisanti, M. P., and Stuehr, D. J. (1998) Interaction between caveolin-1 and the reductase domain of endothelial nitric-oxide synthase. Consequences for catalysis. *J. Biol. Chem. 273*, 22267–22271.

(20) Majumdar, S., Hajduczki, A., Mendez, A. S., and Weiss, G. A. (2008) Phage display of functional, full-length human and viral membrane proteins. *Bioorg. Med. Chem. Lett. 18*, 5937–5940.

(21) Lamboy, J. A., Tam, P. Y., Lee, L. S., Jackson, P. J., Avrantinis, S. K., Lee, H. J., Corn, R. M., and Weiss, G. A. (2008) Chemical and genetic wrappers for improved phage and RNA display. *ChemBioChem 9*, 2846–2852.

(22) Lawrence, M. S., Phillips, K. J., and Liu, D. R. (2007) Supercharging proteins can impart unusual resilience. *J. Am. Chem. Soc. 129*, 10110–10112.

(23) Slovic, A. M., Kono, H., Lear, J. D., Saven, J. G., and DeGrado, W. F. (2004) Computational design of water-soluble analogues of the potassium channel KcsA. *Proc. Natl. Acad. Sci. U.S.A. 101*, 1828–1833.

(24) Kapust, R. B., and Waugh, D. S. (1999) Escherichia coli maltose-binding protein is uncommonly effective at promoting the solubility of polypeptides to which it is fused. *Protein Sci. 8*, 1668–1674.

(25) Matsuura, T., and Pluckthun, A. (2003) Selection based on the folding properties of proteins with ribosome display. *FEBS Lett. 539*, 24–28.

(26) Liu, L., and Pilch, P. F. (2008) A critical role of cavin (polymerase I and transcript release factor) in caveolae formation and organization. *J. Biol. Chem. 283*, 4314–4322.

(27) Hill, M. M., Bastiani, M., Luetterforst, R., Kirkham, M., Kirkham, A., Nixon, S. J., Walser, P., Abankwa, D., Oorschot, V. M., Martin, S.,

Hancock, J. F., and Parton, R. G. (2008) PTRF-Cavin, a conserved cytoplasmic protein required for caveola formation and function. *Cell 132*, 113–124.

(28) Hristova, K., Wimley, W. C., Mishra, V. K., Anantharamiah, G. M., Segrest, J. P., and White, S. H. (1999) An amphipathic alpha-helix at a membrane interface: a structural study using a novel X-ray diffraction method. *J. Mol. Biol. 290*, 99–117.

(29) Bechinger, B. (2000) Understanding peptide interactions with the lipid bilayer: a guide to membrane protein engineering. *Curr. Opin. Chem. Biol. 4*, 639–644.

(30) Brass, V., Bieck, E., Montserret, R., Wolk, B., Hellings, J. A., Blum, H. E., Penin, F., and Moradpour, D. (2002) An amino-terminal amphipathic alpha-helix mediates membrane association of the hepatitis C virus nonstructural protein 5A. *J. Biol. Chem. 277*, 8130–8139.

(31) Yau, W. M., Wimley, W. C., Gawrisch, K., and White, S. H. (1998) The preference of tryptophan for membrane interfaces. *Biochemistry 37*, 14713–14718.

(32) Popot, J. L., and Engelman, D. M. (2000) Helical membrane protein folding, stability, and evolution. *Annu. Rev. Biochem. 69*, 881–922.

(33) Sidhu, S. S., Weiss, G. A. (2002) *Phage Display: A Practical Approach*, Oxford University Press, Oxford.

(34) Chadda, R., and Mayor, S. (2008) PTRF triggers a cave in. *Cell 132*, 23–24.